Supporting information for

Interplay of Hot Carrier Relaxation and Trapping in Red Emissive of Formamidinium Lead Iodide Perovskite Nanorods

*Ankit Kumar [a], Prajit Kumar Singha [a], Aakash Gupta [a], Tapas Pal [a], Sounak Bhattacharya [b], Anindya Datta [a]**

[a] *Department of Chemistry, Indian Institute of Technology Bombay, Powai, Mumbai, India*

[b] *Department of Chemistry, Indian Institute of Technology Kanpur, India*

e-mail: anindya@chem.iitb.ac.in (AD) Phone: +91 22 2576 7149

Table of contents

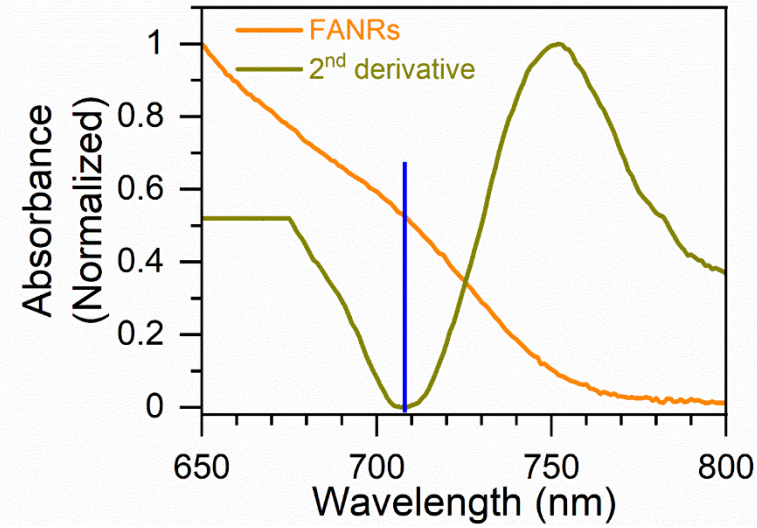

Figure S1 2nd derivative plot of absorbance spectra used to determine the band edge of $FAPbI_3$ NRs

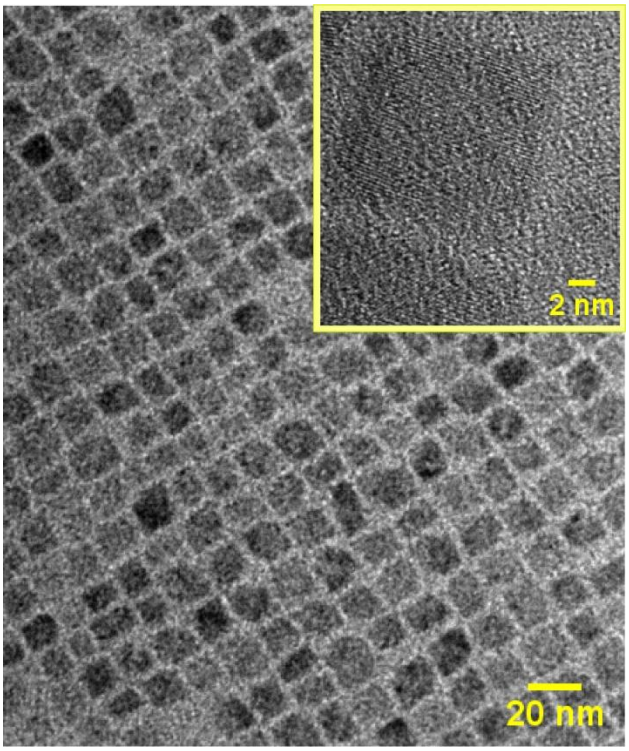

Figure S2 TEM, HRTEM (inset) observed at 120 ^{0}C

Stability and Reproducibility test of $FAPbI_3$ NRs

The nanorods are stable for up to 12 days (Figure 1(a)). It has been observed that with the increasing the number of days absorbance spectra remains identical while PL intensity remains almost similar for 6 days and after that it decreases to 22% compared to the fresh (0 day) data. These nanorods are stored under ambient conditions after the synthesis.

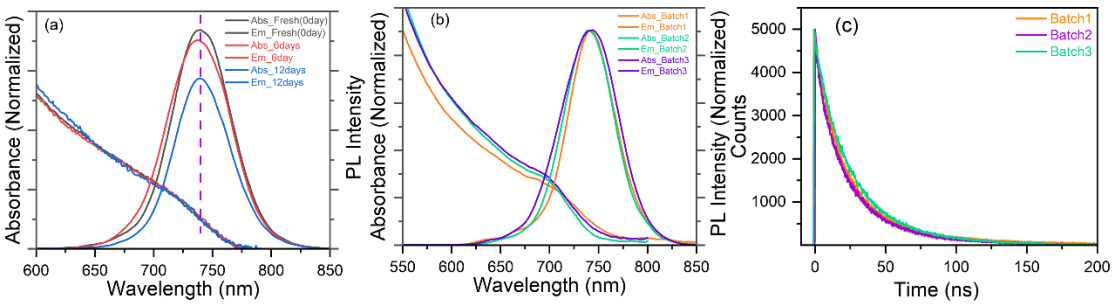

Figure S3 (a) Absorption and emission spectrum recorded for the same sample under ambient conditions, storage up to 12 days with black (fresh (0day), red (6days) and blue (12days),(b) Absorbance and emission recorded for three different batches λ_{ex}= 400 nm, λ_{em}= 740 nm (c)PL recorded for the same set of three different batches as in (b) at λ_{ex}=400 nm collected at λ_{em}= 740 nm.

The synthesis of $FAPbI_3$ NRs has been reproduced several times. The absorption and emission spectra and PL decays have been obtained for three different batches to validate the reproducibility of the $FAPbI_3$ NRs. The band edge remains the identical (~707 nm (Figure 1(a)) and λ_{ex} = 400 nm,λ_{em}^{max}= 740 nm (Figure 1(b)) and PL data collected on λ_{ex}= 400 nm, λ_{em}^{max}= 740 nm (Figure 1(c)). The PL data remains almost identical for all three different batches.

Table S1. TCSPC for $FAPbI_3$ NRs at λ_{ex}= 440 nm and varying λ_{em}= 670 nm to 810 nm

λ_{em}	τ_1 (ns)	a_1	τ_2(ns)	a_2
670	9	0.73	30	0.26
680	9	0.76	30	0.23
690	9	0.78	30	0.21
700	9	0.80	30	0.19
710	9	0.80	30	0.19
720	9	0.81	30	0.18
730	9	0.78	30	0.21
740	9	0.67	30	0.32
750	9	0.55	30	0.44
760	9	0.48	30	0.51
770	9	0.45	30	0.54
780	9	0.48	30	0.51
790	9	0.54	30	0.45
800	9	0.64	30	0.35
810	9	0.75	30	0.24

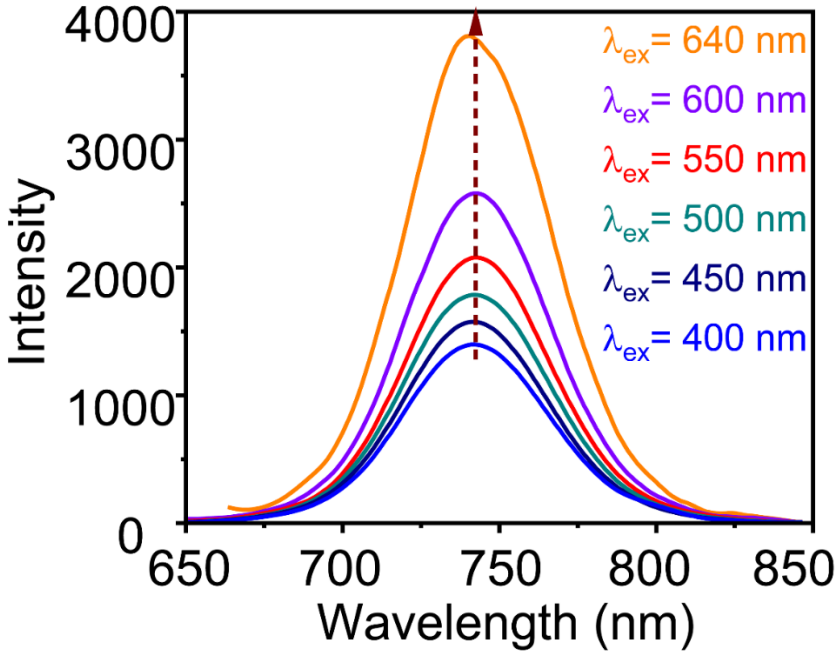

Figure S4 Emission spectra of $FAPbI_3$ NRs from $\lambda_{ex} = 400$ nm to $\lambda_{ex} = 640$ nm.

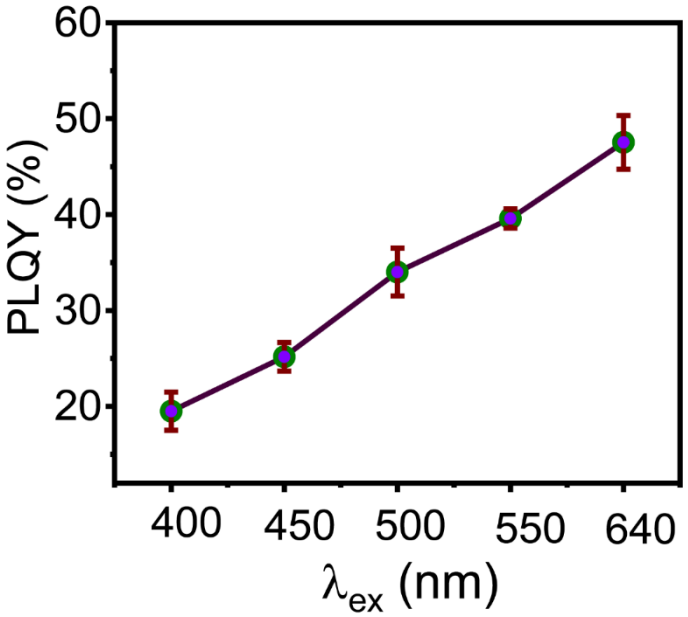

Figure S5 PLQY of $FAPbI_3$ NRs from $\lambda_{ex} = 400$ nm to $\lambda_{ex} = 640$ nm.

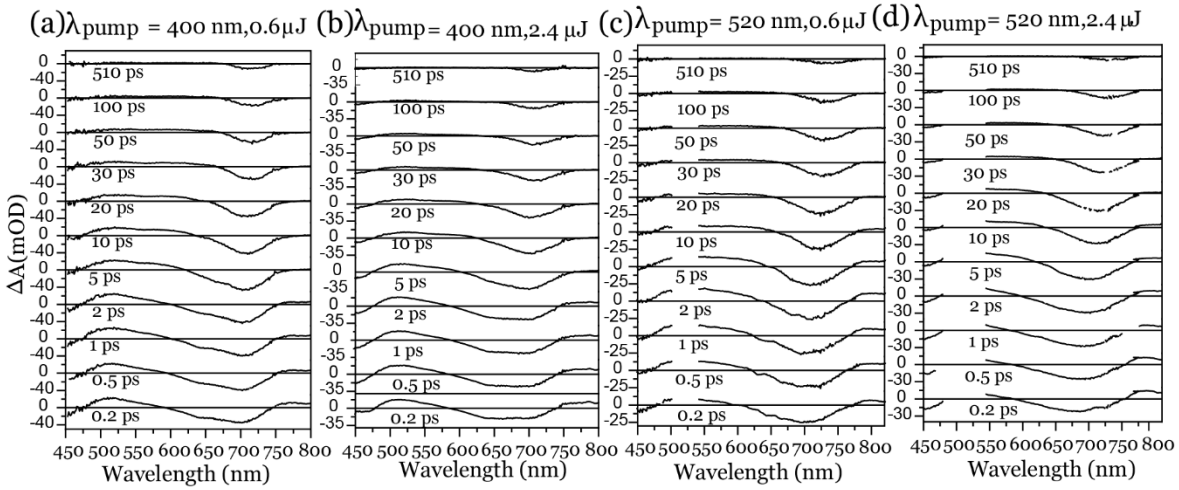

Figure S6 Transient absorption spectra at λ_{pump}= 400 nm and λ_{pump}= 520 nm ((a), (c)) 0.6 μJ,((b),(d)) 2.6 μJ

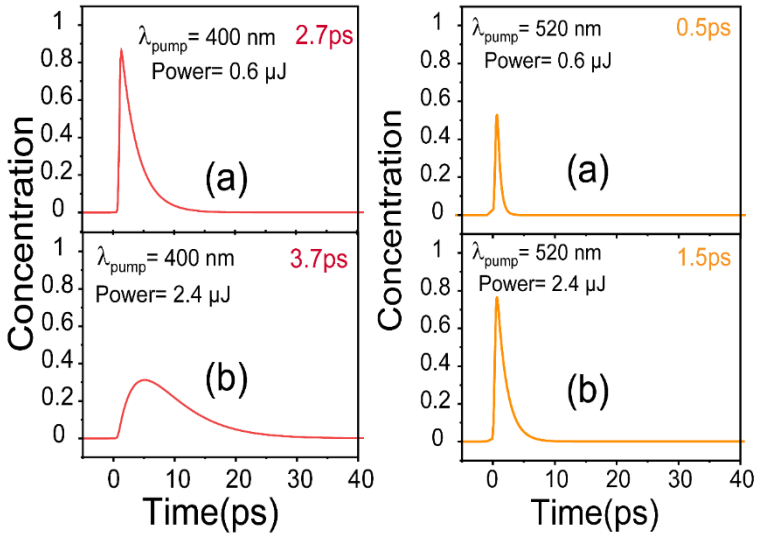

Figure S7 Concentration profile of fast component obtained from SVD at(λ_{pump}= 400 nm (a),(b),red) and (λ_{pump}= 520 nm (a),(b) orange) respectively

Table S2 Hot carrier cooling times for MHPs

System (NCs)	Excitation energy(eV)/ wavelength (nm)	Hot carrier cooling time (τ_{HC}) in ps	Experiment	References
$CsPbCl_3$	350 nm	0.29 ± 0.04	TA	*J. Phys. Chem. C*, **2019**,*123*, 2651 —2657
$CsPbCl_{1.35}Br_{1.65}$	400 nm	0.33 ± 0.02	TA	*ACS Photonics*, **2018**,*5*, 3575 —3583

$CsPbBr_3$	400 nm	0.38-0.42	TA	*Nano Lett.*, **2016**,*16*, 2349 — 2362
$CsPbBr_{1.5}I_{1.5}$	400 nm	0.36-0.38	TA	*Nano Lett.*, **2016**,*16*, 2349 — 2362
$CsPbI_3$	400 nm	0.57-0.58	TA	*Nano Lett.*, **2016**,*16*, 2349 — 2362
$MAPbI_3$ QDs	2.64 eV	0.3	TA	*Adv. Mater.* **2023,** *35* (38), 2301834.
$FAPbI_3$ QDs	2.64eV	0.4	TA	*Adv. Mater.* **2023,** *35* (38), 2301834
$CsPbI_3$ QDs	2.64eV	0.25	TA	*Adv. Mater.* **2023,** *35* (38), 2301834
$FA_{0.5}MA_{0.5}PbI_3$ alloyed QDs	2.64eV	0.45	TA	*Adv. Mater.* **2023,** *35* (38), 2301834
$MA_{0.5}MA_{0.5}PbI_3$ alloyed QDs	2.64eV	0.35	TA	*Adv. Mater.* **2023,** *35* (38), 2301834
$FAPbI_3$ NP	1.96eV	40	TA	*Nanomaterials* **2020,** *10* (10), 1897.
(2D) $CsPbBr_3$ NS (thickness~3 nm)	4.13eV	0.6	TA	*J. Phys. Chem. Lett.* **2020,** *11* (15), 6344-6352.
(3D) $CsPbBr_3$ NS (size~5.5 nm)	4.13eV	>2	TA	*J. Phys. Chem. Lett.* **2020,** *11* (15), 6344-6352.
$CsPbI_3$ NCs	2.48eV	1-20	TA	*Chem. Sci.* **2022,** *13* (6), 1734-1745.
$CsPbI_3$ NCs	2.18eV	0.45-30	TA	*Chem. Sci.* **2022,** *13* (6), 1734-1745.
$CsPbI_3$ NCs	3.1eV	2-30	TA	*Chem. Sci.* **2022,** *13* (6), 1734-1745.
$CsPbBr_3$ NC (size~12 nm)	3.1eV	0.5-1.5	TA	*Adv. Opt. Mater.* **2022,** *10* (9), 2200030.
$CsPbBr_3$ NC (size~12 nm)	3.64eV	0.7	TA	*Adv. Opt. Mater.* **2022,** *10* (9), 2200030.
Cube $CsPbBr_3$ NC	3.1eV	0.9	TA	*J. Phys. Chem. C* **2023,** *127* (18), 8670-8679.
Hexapod $CsPbBr_3$	3.1eV	2	TA	*J. Phys. Chem. C* **2023,** *127* (18), 8670-8679.
$MAPbI_3$ NC	3.1eV	2.5	TA	*J. Phys. Chem. Lett.* **2020,** *11* (7), 2743-2750.
$MAPbBr_3$ NC	3.1eV	1	TA	*J. Phys. Chem. Lett.* **2020,** *11* (7), 2743-2750.
$CsPbBr_3$ NC	3.1eV	0.7	TA	*ChemNanoMat* **2022,** *8* (8), e202200172.
$CsPb(Cl_{0.20}Br_{0.8})_3$ NC	3.1eV	3	TA	*Phys. Rev. B* **2018,** *98* (11), 115418.
$CsPbBr_3$ NCs (size~14 nm)	4.1eV	<0.5	TA	*J. Phys. Chem. Lett.* **2019,** *10* (18), 5302-5311.

$FAPbI_3$ NC (7.5 nm)	$1.25E_g$	0.3	TA	*Nat. Commun.* **2018,** *9* (1), 4197.
$FAPbI_3$ NC (12.9 nm)	1.25Eg	0.25	TA	*Nat. Commun.* **2018,** *9* (1), 4197.
$FAPbI_3$ NRs (length=57.4 ±1.3 nm, diameter= 32.1 ± 0.3 nm).	400 nm	τ_1= 2.7-3.7, τ_2= 8.1-5.1	TA	*This work*
	520 nm	τ_1= 0.5-1.5, τ_2= 8.2-13.07	TA	

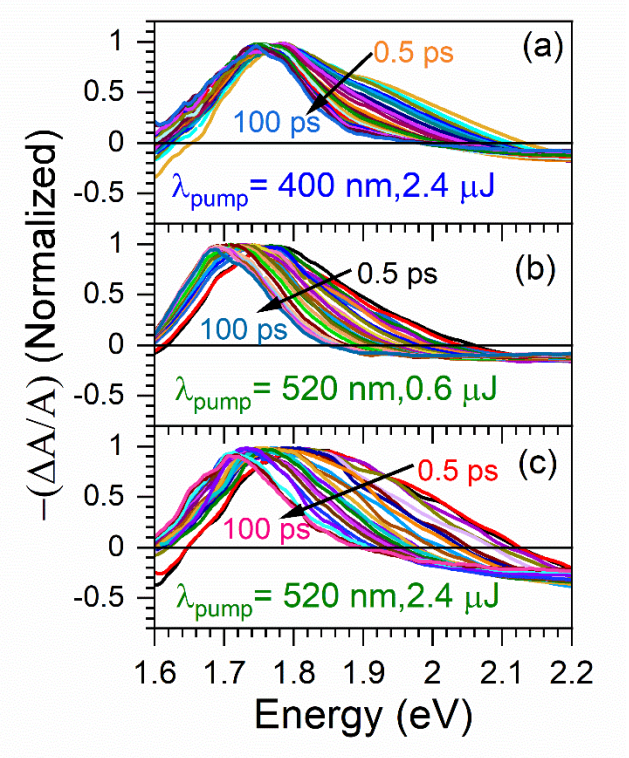

Figure S8 Transient absorption spectra (inverted plotted in energy domain and normalized at the spectral maximum) at λ_{pump} = 400 nm (a) and λ_{pump} = 520 nm (b),(c). The arrows indicate the high-energy tail region used for Maxwell-Boltzmann (MB) fitting.

Note SN1 Decay – Associated Emission spectra [1]

Suppose a sample displays a multi-exponential decay, and that the decay is different at different emission wavelengths. The intensity decay is then described by

$$I(\lambda, t) = I(t) = \sum_i a_i(\lambda) \exp\left(^{-t}/_{\tau_i}\right)$$

Where $a_i(\lambda)$ are the wavelength-dependent pre-exponential factors and the τ_i decay times. This expression assumes the decay times are independent of wavelengths. The emission spectrum due to each component can be calculated using

$$I_i\,(\lambda) = \frac{a_i(\lambda)\tau_i I(\lambda)}{\sum_j a_j(\lambda)\tau_j}$$

In this expression $I(\lambda)$ is the steady-state emission spectrum. The product $a_i(\lambda)\tau_i$ appears in the numerator because the steady–state intensity is proportional to this product. The sum in the denominator is proportional to the total intensity at this wavelength. The spectra $I_i\,(\lambda)$ are called decay-associated spectra (DAS) because they represent the emission spectrum of the component emitting with a lifetime τ_i. The multi-exponential decays collected for each emission wavelength are used to construct the emission spectra associated with each decay.

Note SN 2 Singular value decomposition (SVD) for global fitting

SVD combined with global fitting is an effective analytical method for complex spectra with overlapping features.[2] Using this analysis, the main components from the original data are extracted, remove the unnecessary components, and then reasonably analyze the extracted principal components to obtain the spectrum and kinetic curves of the transient components and filter out the experimental noise.[3] The measured TA data are a two- dimensional matrix A consisting of m_λ wavelengths and n_t times. Any one of the elements in matrix A can be expressed as follows

$$A_{ij} = A(\lambda_i, t_j)$$

For matrix A of real elements, SVD is defined by the product of three matrices, called the SVD of A

$$A = UST^V$$

Where the column vectors of U and V are referred to as the left and right singular vectors of A, respectively, S is the singular value of the SVD transient components, and U contains the basis spectra of the data matrix A

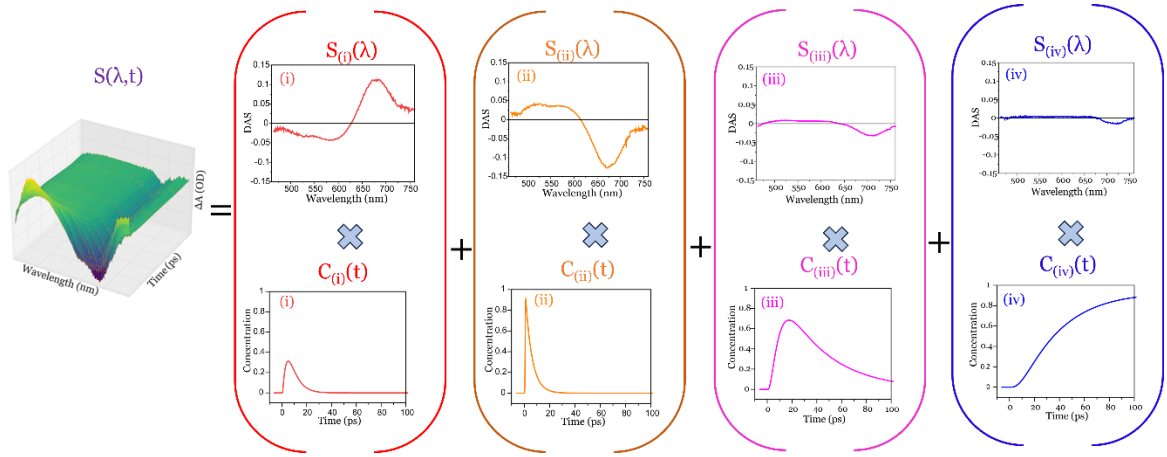

Figure S9 Global analysis representation of transient absorption spectroscopy data (TAS) (left-hand side) gives decay-associated spectra (right-hand side) with their respective coefficients generated using Singular value decomposition (SVD). S(λ,t) is experimental TAS data, which is decomposed into four components from ($S_{i=1\ to\ 4}(\lambda)$) and their concentration profile ($C_{i=1\ to\ 4}(t)$).

Note SN 3 Calculation of power density of fs Transient absorption spectroscopy[4,5]

All the data has been measured at the high (1.2 mW) and low pump (0.3 mW) fluence respectively, with the repetition rate 500 Hz after the chopper.

The energy per pulse in low pump fluence at the sample, $E_{Pulse} = \frac{0.3\ mW}{500\ s^{-1}} = 0.6\ \mu J$

The energy per pulse in high pump fluence at the sample, $E_{Pulse} = \frac{1.2\ mW}{500\ s^{-1}} = 2.4\ \mu J$

The laser beam diameter $(2r)$= 500 µm

The area of the pump pulse at the sample (A)= $\pi r^2 = \pi(0.025)^2 cm^2 = 0.002 cm^2$

The low pump fluence = $\frac{E_{Pulse}}{A} = \frac{0.6}{0.002}\mu J/cm^2 = 0.3\ mJ/cm^2$

The high pump fluence = $\frac{E_{Pulse}}{A} = \frac{2.4}{0.002}\mu J/cm^2 = 1.2\ mJ/cm^2$

Note SN 4 Average exciton occupancy (<N>) calculation[6]

Average exciton occupancy is directly calculated from magnitude of GSB signal by the equation:

$$\left|\frac{\Delta A}{A}\right|_{1S} = 1 - e^{-<N>}(1 + \frac{< N >}{2})$$

Average exciton occupancy follows Poisson distribution:

$$P(N) = < N >^{N} \frac{e^{-<N>}}{N!}$$

Where <N> is the average number of exciton and $P(N)$ is the probability of having N exciton. At high fluence intensity of bleach signal is affected due to the The concomitant GSB buildup and PIA decay is assigned to the arrival of the carriers at the band edge during the initial thermalization and relaxation.[7–9] To consider all those factors into account the average exciton occupancy have calculated from above equation for the lower excitation intensity. At low fluence $< N_0 >$ i.e., the number of excitons at time zero is defined as

$$< N_0 > = \sigma J_p$$

Where σ is the absorption cross-section and J_p is the photon flux per pump pulse. <N> at high power is calculated from the equation:

$$\frac{< N >_1}{E_1} = \frac{< N >_2}{E_2}$$

Table.S3 Average exciton occupancy <N> in $FAPbI_3$ NRs at different pump power.

Energy (μJ)	$< N >_{pump=400\ nm}$	$< N >_{pump=520\ nm}$
0.6	0.02	0.01
2.4	0.08	0.05

References

(1) *Principles of Fluorescence Spectroscopy*; Lakowicz, J. R., Ed.; Springer US: Boston, MA, 2006.

(2) Schmidt, M.; Rajagopal, S.; Ren, Z.; Moffat, K. Application of Singular Value Decomposition to the Analysis of Time-Resolved Macromolecular X-Ray Data. *Biophys. J.* **2003**, *84*, 2112–2129.

(3) Narra, S.; Jokar, E.; Pearce, O.; Lin, C.-Y.; Fathi, A.; Diau, E. W.-G. Femtosecond Transient Absorption Spectra and Dynamics of Carrier Relaxation of Tin Perovskites in the Absence and Presence of Additives. *J. Phys. Chem. Lett.* **2020**, *11*, 5699–5704.

(4) Li, L.; Pandey, A.; Werder, D. J.; Khanal, B. P.; Pietryga, J. M.; Klimov, V. I. Efficient Synthesis of Highly Luminescent Copper Indium Sulfide-Based Core/Shell Nanocrystals with Surprisingly Long-Lived Emission. *J. Am. Chem. Soc.* **2011**, *133*, 1176–1179.

(5) Eliasson, N.; Rimgard, B. P.; Castner, A.; Tai, C.-W.; Ott, S.; Tian, H.; Hammarström, L. Ultrafast Dynamics in Cu-Deficient CuInS 2 Quantum Dots: Sub-Bandgap Transitions and Self-Assembled Molecular Catalysts. *J. Phys. Chem. C* **2021**, *125*, 14751–14764.

(6) Das, S.; Rakshit, S.; Datta, A. Interplay of Multiexciton Relaxation and Carrier Trapping in Photoluminescent CdS Quantum Dots Prepared in Aqueous Medium. *J. Phys. Chem. C* **2020**, *124*, 28313–28322.

(7) Han, X.; Huang, Z.; Zhang, G.; Yang, C.; Li, J.; Zhang, M.; Chen, Z.; Wang, J.; Chen, R.; Qin, C.; Hu, J.; Yang, Z.; Liu, X.; Wang, Y.; Ma, J.; Xiao, L.; Jia, S. Ultrafast Exciton Formation in Perovskite Quantum Rods. *Nano Lett.* **2025**, *25*, 4913–4920.

(8) Wang, X.; Huo, D.; Wang, X.; Li, M.; Wang, Y.; Wan, Y. Hot Carrier Dynamics and Charge Trapping in Surface Passivated β-CsPbI 3 Inorganic Perovskite. *J. Phys. Chem. Lett.* **2021**, *12*, 6907–6913.

(9) Chen, J.; Messing, M. E.; Zheng, K.; Pullerits, T. Cation-Dependent Hot Carrier Cooling in Halide Perovskite Nanocrystals. *J. Am. Chem. Soc.* **2019**, *141*, 3532–3540.